Beacon: A Naturalistic Driving Dataset During Blackouts for Benchmarking Traffic Reconstruction and Control

Supriya Sarker, Iftekharul Islam, Bibek Poudel, and Weizi Li

Abstract— Extreme weather and infrastructure vulnerabilities pose significant challenges to urban mobility, particularly at intersections where signals become inoperative. To address this growing concern, we introduce Beacon, a naturalistic driving dataset capturing traffic dynamics during blackouts at two major intersections in Memphis, TN, USA. The dataset provides detailed traffic movements, including timesteps, origin, and destination lanes for each vehicle over four hours of peak periods. We analyze traffic demand, vehicle trajectories, and density across different scenarios, demonstrating high-fidelity reconstruction under unsignalized, signalized, and mixed traffic conditions. We find that integrating robot vehicles (RVs) into traffic flow can substantially reduce intersection delays, with wait time improvements of up to 82.6%. However, this enhanced traffic efficiency comes with varying environmental impacts, as decreased vehicle idling may lead to higher overall CO_2 emissions. To the best of our knowledge, Beacon is the first publicly available traffic dataset for naturalistic driving behaviors during blackouts at intersections.

I. INTRODUCTION

Modern urban infrastructure is vulnerable to increasing extreme weather events and other disturbances. These factors can lead to power outages, incapacitating critical urban systems, with traffic control mechanisms being significantly affected [1]. Traffic lights, the backbone of urban traffic management, are entirely dependent on electricity. Thus, their failure during blackouts will result in gridlocks and increased accident risks, especially at the intersections, where over 45% of traffic crashes in the U.S. occur [2]. During blackouts, intersections can remain uncontrolled for extended periods, causing widespread congestion and crash hotspots in a city [3], [4]. To address these challenges and develop effective traffic management solutions during blackouts, datasets that capture real-world traffic behavior during power outages are essential. However, collecting this type of data requires naturally occurring blackouts, as deliberately creating a blackout for data collection is impractical and unsafe.

In response to this critical need, we introduce Beacon, a dataset containing four hours of traffic dynamics during peak hours (midday and afternoon), captured during a blackout in Memphis, TN, USA. Beacon provides detailed traffic movements at two real-world intersections shown in Fig. 1, offering information such as the time, origin, and destination lanes of all vehicles. This naturalistic driving dataset presents a unique opportunity to study and

Supriya Sarker, Iftekharul Islam, Bibek Poudel, and Weizi Li are with Min H. Kao Department of Electrical Engineering and Computer Science at University of Tennessee, Knoxville, TN, USA {ssarker8,mislam73,bpoudel3}@vols.utk.edu; weizili@utk.edu
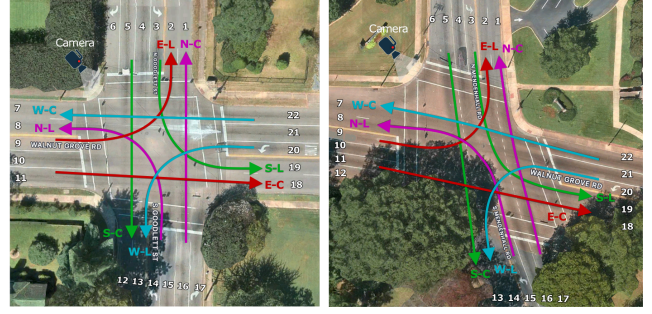
Fig. 1. Top-down views of the two intersections in Memphis, TN, USA where blackouts occurred and data was captured. Lane numbering and traffic flow directions are also shown.

analyze traffic behaviors at complex intersections during blackouts. Beacon can be obtained at https://github.com/Fluidic-City-Lab/Beacon_dataset.

Traffic reconstruction has gained significant attention in intelligent transportation research [5], enabling the analysis of microscopic patterns like stop-and-go waves [6] and macroscopic dynamics like citywide congestion propagation [7]. Unlike most datasets that capture general road conditions without considering rare disruptions [8]–[10], our work presents the first real-world dataset and analysis of unsignalized intersection traffic during blackouts, offering three key contributions:

- We introduce Beacon—a driving dataset enabling analysis of natural driver behaviors and adaptation at real-world, unsignalized intersections.
- We demonstrate Beacon's utility through high-fidelity traffic reconstruction under three cases: unsignalized conditions during blackout, signalized conditions after power restoration, and mixed traffic control with both human-driven and robot vehicles (RVs).
- Our analysis reveals various key insights about traffic behavior and control strategies during infrastructure disruptions: (1) RVs can effectively coordinate traffic flow, reducing wait times by up to 82.6%; (2) the effectiveness of traffic management strategies depends on traffic demand, with high-demand intersections benefiting more from automated coordination; and (3) while introducing RVs improves efficiency, their impact on emissions varies—reducing idle time but potentially increasing overall CO_2 output.

By providing both a benchmark dataset and comprehensive analysis across different reconstruction and control strategies, we aim to accelerate research in traffic resilience, autonomous vehicle coordination, and the development of intelligent

transportation systems that can maintain efficient flow during infrastructure disruptions. Our findings highlight the need for adaptive deployment strategies that balance traffic efficiency with environmental considerations, while our benchmarking framework enables systematic evaluation of such strategies.

II. RELATED WORK

A. Traffic Datasets and Simulation

Real-world traffic datasets are essential for developing and validating simulation environments that reflect diverse traffic conditions. Shen et al. [11] analyze two decades (2001–2021) of traffic collision reconstruction using tools like CiteSpace, VOSviewer, and SciMAT. Li et al. propose ScenarioNet [12], an open-source platform for large-scale traffic scenario modeling and simulation for autonomous driving. It aggregates and standardizes data from real-world sources such as Waymo [13], nuScenes [14], and Argoverse [15]. Another contribution by Li et al., MetaDrive [16], supports both single- and multi-agent reinforcement learning in procedurally generated environments. It integrates diverse sensor modalities, including LiDAR, RGB, semantic maps, and first-person views. Amini et al. present VISTA 2.0 [17], a data-driven simulator designed to improve perception-to-control robustness by synthesizing realistic multi-sensor data (e.g., RGB, 3D LiDAR, event cameras) from high-fidelity datasets. Furthermore, AWSIM [18] is a 3D simulation platform for Autoware, enabling realistic AV testing using LiDAR and other sensors. It supports dynamic traffic with pedestrians and vehicles, allowing evaluation of decision-making and safety in complex environments.

B. Traffic Reconstruction and Control

Traffic reconstruction and control are central to transportation engineering. Sanchez et al. [6] use the Caltrans PeMS dataset to implement a kernel-based method that identifies stop-and-go events and congestion hotspots. Bilotta and Nesi [19] propose a model that resolves traffic data indeterminacy by solving partial differential equations (PDEs) and estimating junction flow using real-time sensor inputs. Qi et al. [20] reconstruct vehicle trajectories using ALPR data, applying travel-time-based trip segmentation, a modified K-shortest-path algorithm, and auto-encoder-based trajectory selection. Bakowski and Radziszewski [21] assess the effects of road reconstruction on traffic and noise, finding that noise levels can drop even with increased vehicle volume, offering insight into environmental impacts of urban modifications.

Recent traffic control approaches incorporate autonomous vehicles as dynamic control agents. Čičić et al. [22] use CAVs as mobile sensors and actuators, estimating local traffic density and controlling congestion by dissipating stop-and-go waves through simulation. Mixed traffic control—managing interactions between AVs and HVs—has gained traction as a promising solution to urban traffic challenges. Wu et al. [23] show that AVs can dampen stop-and-go waves to stabilize traffic, while Peng et al. [24] and Yan and Wu [25] demonstrate how CAVs enhance intersection throughput and reduce conflicts. Wang et al. [26], [27] develop a decentralized

control framework that significantly lowers waiting times at unsignalized intersections. Villarreal et al. [28] utilize image-based observations, and Poudel et al. [29], [30] improve reliability by incorporating real driving profiles. Islam et al. [31] validate the potential of heterogeneous mixed traffic control to enhance efficiency and cut emissions across varied traffic settings.

III. DATA COLLECTION AND ANALYSIS

A. Data Collection

Beacon provides a valuable benchmark for urban traffic analysis by focusing on two intersections with characteristic four-way layouts on major arterial roads [8], [32]. It contains 4 hours of traffic data collected during a blackout on July 19, 2023, from two Memphis, TN intersections shown in Fig. 1: Walnut Grove-Goodlett St. (lat: 35.1315, lon: -89.9255) and Walnut Grove-Mendenhall Rd. (lat: 35.1308, lon: -89.8985). We manually annotate the dataset by carefully examining the recorded videos. To distinguish time and location, we use WGG-N and WGG-AN to refer to Walnut Grove-Goodlett at noon (12 PM–1 PM) and afternoon (5 PM–6 PM), respectively. Similarly, WGM-N and WGM-AN denote Walnut Grove-Mendenhall during the same time intervals.

To validate the sufficiency of the one-hour data, we analyze the statistical stability of traffic throughput. The plots in Fig. 2 show the cumulative average of vehicle arrivals per minute, which converge to a stable mean for all scenarios, with the minor exception of a final dip in the WGM-N case caused by a brief lull of traffic. This convergence confirms that the one-hour period is sufficient to establish a representative baseline of intersection performance.

B. Data Analysis

We analyze Beacon in terms of the traffic demand and vehicle trajectories across all scenarios.

1) Traffic Demand: Table I shows the traffic demand for each scenario, broken down by direction. The data reveals variations in traffic volume and directional flow across different times and locations. WGG-N sees the lowest demand with 1,983 vehicles, while the same intersection experiences the highest demand 2,453 vehicles during the afternoon peak hour, i.e., WGG-AN. At a different intersection, WGM-N experiences less demand during noon with 2,033 vehicles compared to WGM-AN which has the demand 2,342 vehicles
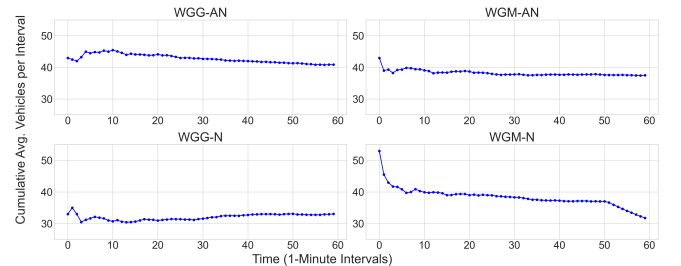

Fig. 2. Statistical stability of traffic flows across all scenarios. The cumulative average throughput quickly converges to a stable mean, demonstrating that the traffic reaches a steady state. This validates that the one-hour data collection period is representative of intersection dynamics.

during the afternoon peak hour. The directional patterns also differ at the two intersections. At WGG, eastbound traffic dominates, while at WGM, westbound traffic is predominant.

2) Vehicle Trajectory: Both intersections demonstrate strong east-west traffic flows along Walnut Grove Road, indicating its role as a major arterial route. At WGG, the most significant movements during afternoon are westbound-straight (248 vehicles) and eastbound-straight (228 vehicles). WGM, on the other hand, exhibits more balanced east-west flows, with consistent traffic volumes throughout the day.

While at both intersections, proceeding straight is the most common maneuver, other turning behaviors vary by direction and location. At WGG, we notice a strong preference for northbound right turns over left turns in both scenarios, while southbound left turns outnumber right turns. The pattern differs at WGM, where northbound left turns significantly surpasses right turns in both scenarios. These differences in turning preferences are likely linked to the surrounding road network, and the destinations accessible from each turn.

IV. Traffic Reconstruction

Using Beacon, we first reconstruct traffic during the data collection period—enabling various traffic engineering applications for analyzing vehicle behavior at complex intersections during blackouts.

We obtain the road networks of WGG and WGM from OpenStreetMap (OSM) [33] and convert them into simulation-ready formats using SUMO's NETCONVERT tool [34]. During conversion, we preserve key OSM road attributes such as lane counts, intersection layouts, and geometries. From Beacon, we extract each vehicle's start lane, end lane, and the timestep when it reaches the head of its starting lane to form its route. This information is then used in SUMO to simulate and reconstruct traffic flow. Fig. 3 illustrates the reconstructed scenarios: WGG-N (top left), WGG-AN (top right), WGM-N (bottom left), and WGM-AN (bottom right).

To evaluate the accuracy of our traffic reconstruction, we compare the reconstructed traffic in SUMO with the recorded data. We focus on three types of potential mismatch: **start lane**, which refers to the vehicle's departure lane; **end lane**, the arrival lane of a vehicle; and **timestep**, which captures differences in vehicle timing at the head of the start lane. The evaluation results are provided in Table II. First, no mismatches are found with respect to the start
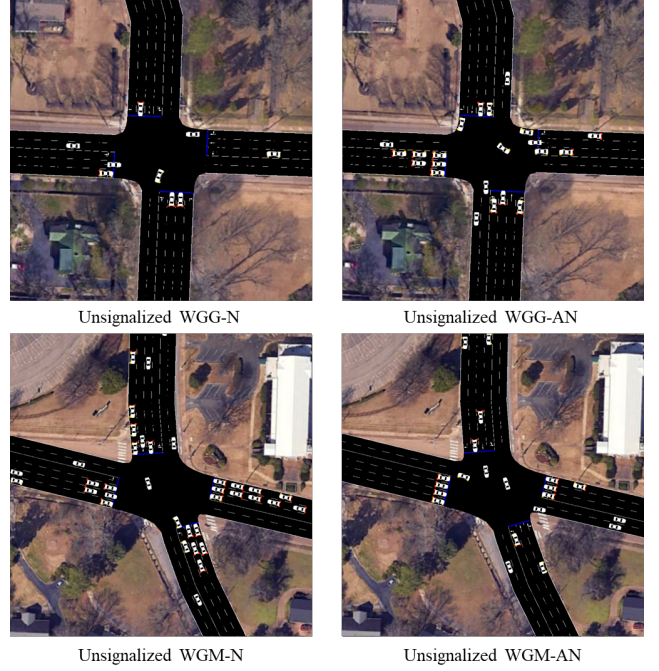

Fig. 3. Traffic reconstruction via the Beacon dataset demonstrating vehicle behaviors at complex intersections during blackouts.

lane, indicating that all vehicles depart from the correct lane. However, discrepancies are observed in both the end lane and timesteps. These inconsistencies arise because SUMO's vehicle generation process may not follow the imported data exactly, even when vehicle timestep information is documented accurately in the route file. In addition, upon exiting the intersection, some vehicles chose a different arrival lane compared to imported data. This is due to SUMO's internal lane-changing mechanisms, which is beyond our control. Despite these differences, our reconstruction achieves high accuracy, with match rates exceeding 98% at WGG. Although WGM shows slightly lower accuracy due to end lane mismatches, it still maintains match rates above 91%. While trajectory-based metrics (e.g., RMSE, path deviation) offer finer-grained evaluations, they require continuous per-frame vehicle positions, which are unavailable in our dataset. Our evaluation metrics instead focus on route-level correctness and timing consistency—practical proxies that reflect key spatiotemporal behaviors relevant to intersection dynamics.

V. Signalized Intersections

After analyzing blackout scenarios, we next study traffic at the same intersections with signal control. This comparison

TABLE I

The traffic demands of all four scenarios in Beacon are shown. WGG and WGM represent two different intersections, respectively. N represents noon (12PM–1PM) and AN represents afternoon (5PM–6PM). The largest demands at various directions are highlighted.

Scenario	North-bound	South-bound	East-bound	West-bound	Total Demand
WGG-N	280	410	**685**	608	1,983
WGG-AN	425	629	**794**	605	2,453
WGM-N	403	434	527	**669**	2,033
WGM-AN	494	523	625	**700**	2,342

TABLE II

Comparing traffic reconstruction with recorded data. Our reconstruction demonstrates high accuracy, maintaining match rates above 91% across all scenarios.

Scenario	#vehicles	Start lane mismatch	End lane mismatch	Timestep mismatch	Total mismatch	Match rate (%)
WGG-N	1,962	0	38	0	38	98.07
WGG-AN	2,452	0	10	0	10	99.59
WGM-N	2,032	0	5	191	196	91.60
WGM-AN	2,342	0	6	199	205	91.25

offers insights into effective traffic management at complex intersections. Additionally, incorporating traffic signal phase information for WGG and WGM enriches the dataset.

Once power was restored, we recorded traffic light behavior from all approaches at both intersections and extracted their phase sequences, shown in Fig. 5. At WGG, the sequence repeats as 7, 4, 29, 4, 20, 4, 4, 40, and 4 seconds; for WGM, it is 22, 4, 80, 4, 42, 4, 4, 113, and 4 seconds. Each phase controls green, yellow, and red lights for specific directions, ensuring orderly flow.

We simulate these signalized scenarios in SUMO using the same traffic input as Beacon, with examples shown in Fig. 4. Although both blackout and signalized cases use SUMO's default IDM model [35], we observe key differences. In blackout scenarios, vehicles self-organize to avoid collisions, often leaving space at intersections. With traffic lights, vehicles must stop during red phases, resulting in longer queues. Additionally, signal control enforces turn priority—right turns always have precedence over left turns—whereas blackout traffic treats all directions with equal priority.

To quantitatively assess these differences, we compare three key metrics in Table III: average wait time, travel time, and CO_2 emissions. Wait time reflects how long vehicles are delayed at the intersection; travel time is the average trip duration; and emissions are computed using SUMO's HBEFA3-based model [36], with vehicles classified as "PC_G_EU4" passenger cars. Across all scenarios, blackout (unsignalized) operation consistently reduces delay, with lower travel and wait times than fixed-time signals. This result suggests that self-organizing human behavior can outperform pre-timed signals, especially in low to moderately loaded intersections. However, emissions trends are more nuanced. In three scenarios with moderate demand, blackout also yields lower emissions by avoiding the stop-and-go cycles of signal control. Conversely, in the highest-demand scenario (WGG-AN), the efficiency likely requires more frequent and aggressive vehicle accelerations to maintain throughput, an emission-intensive driving cycle that results in higher overall CO_2 emissions. This highlights a fundamental trade-off, demonstrating that optimizing for traffic delay does not guarantee a corresponding environmental benefit.

To validate our simulation, we compare it with the recorded traffic data. Since traffic lights alter vehicle timing, we focus the evaluation on start and end lanes. Results are shown in Table IV. All scenarios achieve over 84% accuracy, with WGG performing nearly perfectly. Compared to blackout reconstruction, signalized simulations show slightly higher end-lane mismatches. This occurs because red lights cause vehicle queues that are released in bursts, leading to end-lane congestion. SUMO's internal lane-changing logic may redirect vehicles to less crowded lanes, resulting in mismatches. The mismatch is more pronounced at WGM due to its complex geometry. Factors such as more lanes, skewed intersection angles, and crosswalks contribute to higher collision risk [37]. While real drivers navigate cautiously and stay in-lane, SUMO may reroute vehicles to perceived safer lanes, increasing end-lane deviations.

TABLE III

PERFORMANCE COMPARISON OF SIGNALIZED VS. UNSIGNALIZED (BLACKOUT) CONTROL. WHILE THE UNSIGNALIZED BLACKOUT OPERATION CONSISTENTLY YIELDS SUPERIOR TRAVEL AND WAIT TIMES ACROSS ALL SCENARIOS, IT REVEALS A CRITICAL TRADE-OFF WITH ENVIRONMENTAL IMPACT, LEADING TO HIGHER CO_2 EMISSIONS IN THE HIGH-DEMAND WGG-AN SCENARIO.

Scenario	Control	Avg Travel Time (s)	Avg Waiting Time (s)	CO_2 per timestep (mg)
WGG-N	Signalized	97.86	17.82	2360.11
	Blackout	82.48	1.91	2304.54
WGG-AN	Signalized	66.75	16.51	4191.62
	Blackout	53.35	1.96	4716.11
WGM-N	Signalized	134.25	46.55	2399.35
	Blackout	116.22	16.40	2303.23
WGM-AN	Signalized	136.35	48.11	2400.33
	Blackout	123.36	20.05	2306.93

Signalized WGG-N   Signalized WGG-AN
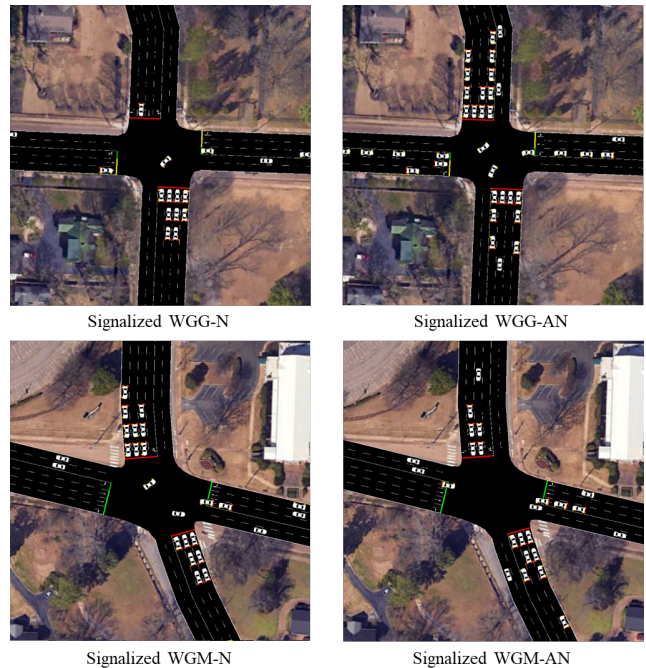
Signalized WGM-N   Signalized WGM-AN

Fig. 4. Traffic simulation using the Beacon dataset as input at signalized intersections WGG and WGM.

VI. MIXED TRAFFIC CONTROL

Using Beacon as a benchmark, we evaluate advanced control strategies at real-world WGG and WGM intersections. As a case study, we examine mixed traffic control where robot vehicles (RVs) coordinate with human-driven vehicles (HVs) to optimize flow. Building on Wang et al. [26], we assess RV control effectiveness using unsignalized traffic data—providing insights for future RV-integrated systems.

Mixed traffic control can be modeled as a multi-agent reinforcement learning problem, where RVs act as independent agents in a partially observable environment. The system is formulated as a Partially Observable Markov Decision Process (POMDP), defined by the tuple $(S, A, T, R, O, Z, \delta)$, where S is the traffic state (e.g., positions, velocities), A the action space for each RV, and $T(s'|s, a)$ the state transition

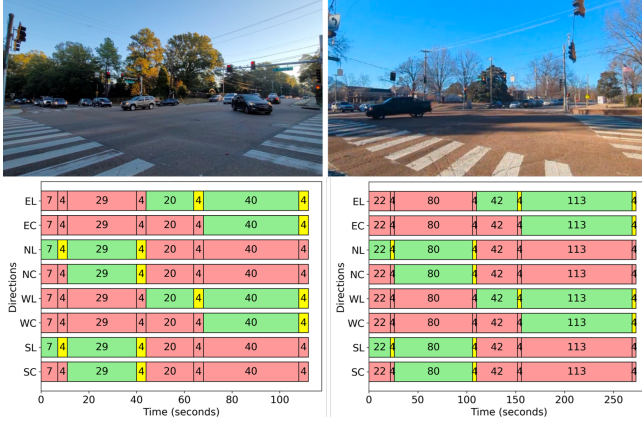| Scenario	#vehicles	Start lane mismatch	End lane mismatch	Total mismatch	Match rate (%)
WGG-N	1,961	0	12	12	99.39
WGG-AN	2,135	0	96	96	95.51
WGM-N	2,031	0	287	287	85.87
WGM-AN	2,340	0	369	369	84.23

Fig. 5. Top: Photographs of the Walnut Grove-Goodlett (left) and Walnut Grove-Mendenhall (right) intersections captured during regular traffic conditions with functional traffic lights. Bottom: Corresponding signal timing phases of the traffic lights at the two intersections.

function. The reward function $R(s,a)$ reflects objectives such as reduced wait time and improved throughput. Due to partial observability, each RV accesses O with observation probabilities $Z(o|s)$. Each agent follows a policy $\pi_\phi(a_t|s_t)$ to select actions that maximize the cumulative discounted reward $R_t = \sum_{i=t}^{T} \delta^{i-t} r_i$, with discount factor $\delta \in [0,1)$. This framework enables RVs to learn effective strategies under uncertainty from human-driven behavior.

In our implementation, the action space A is a discrete 'Stop/Go' command set. HVs are governed by the Intelligent Driver Model (IDM). RVs use a hybrid policy, executing 'Go' (max acceleration) or 'Stop' ($a = -u^2/2d_{int}$, based on speed u and distance d_{int}) actions within 30m of the intersection, while defaulting to IDM otherwise. The reward function $R(s,a)$ is designed to improve throughput and reduce delays. The observation $o_t \in O$ is a vector of local traffic states including queue lengths, wait times, intersection occupancy, and the RV's own distance to the intersection. We train a single, shared policy using Rainbow DQN [38] with a 3-layer MLP (512 units/layer), trained for 1,000 iterations with a learning rate of 5×10^{-4} and a discount factor $\delta = 0.99$. Fig. 6 shows reconstructed mixed traffic using Beacon, where red vehicles are RVs and white vehicles are HVs. Each scenario has 60% RV penetration rate, but any penetration rate in the range [0, 100] can be selected.

To evaluate mixed traffic control performance, we analyze metrics from 1000-second simulations. Table V shows that RV effectiveness depends on traffic volume. At the simpler WGG
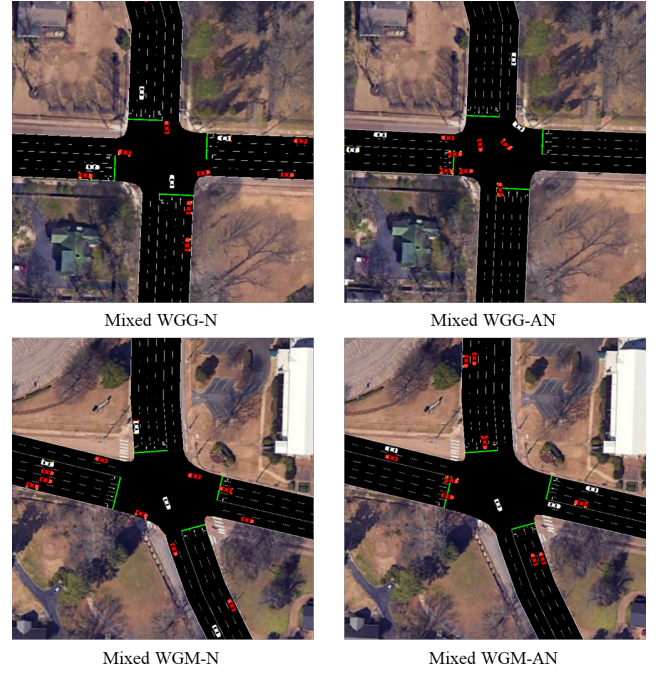
Fig. 6. Reconstructed mixed traffic using Beacon: (a) WGG-N, (b) WGG-AN, (c) WGM-N, (d) WGM-AN. Red = robot vehicles (RV), white = human-driven vehicles (HV), with 60% RV penetration. Reconstruction enables RVs to learn actions that improve traffic efficiency.

intersection, RVs provide minimal benefit under low traffic, suggesting that coordination is not critical when demand is low. In contrast, at the more complex WGM intersection, RVs significantly reduce both wait and travel times, particularly during high-traffic periods. Figure 7 visualizes these trends across RV penetration rates for all four scenarios. In WGG-N, low density leads to minimal congestion, limiting the potential gains from RVs. At WGM, however, higher penetration (80–100%) yields noticeable performance improvements under heavier traffic. While wait times at WGM are lower (Fig. 7, left), travel times remain higher due to the intersection's skewed geometry. As discussed earlier, cautious driving behavior in WGM leads to slower navigation, explaining the longer travel times in both WGM-N and WGM-AN. Regarding emissions, CO_2 outcomes vary. In WGG-N, low density naturally leads to lower emissions. In WGM scenarios, RVs help reduce emissions by minimizing stop-and-go patterns. However, in WGG-AN, emissions rise despite lower delays. This is because RVs increase throughput under heavy demand by accelerating more frequently to maintain flow, which results in higher per-vehicle energy use. This highlights a key trade-off: reducing delays doesn't always translate to lower emissions, especially when demand levels require aggressive acceleration to sustain efficiency.

To further investigate the traffic volume threshold hypothesis, we conduct additional simulations at the WGG intersection, increasing the traffic demand at each direction from WGG-AN by 25% and 50%. Table VI presents the results. With a 25% demand increase, we observe that incorporating RVs reduces wait times by upto 82.6% and travel time by 10.3%. However, this improvement comes
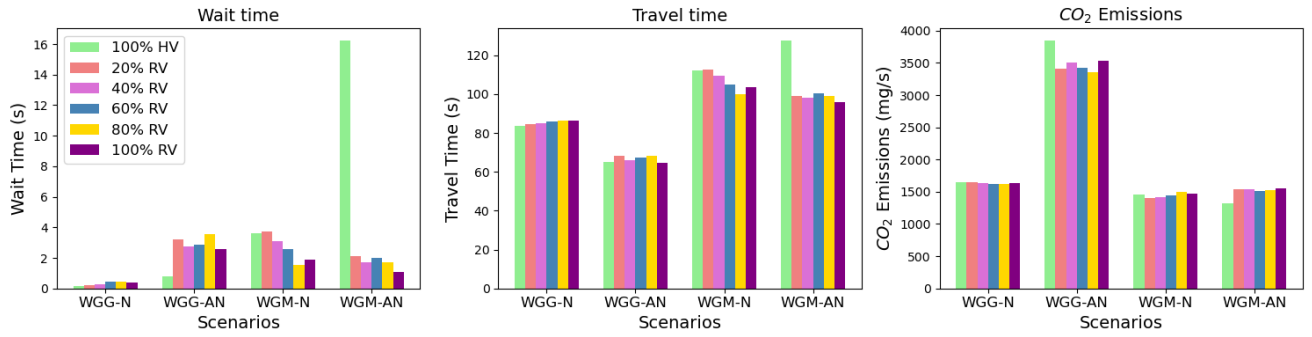
Fig. 7. Comparison of wait time (left), travel time (center), and CO_2 emissions (right) across four scenarios (WGG-N, WGG-AN, WGM-N, WGM-AN) under different RV penetration rates. RVs significantly reduce wait times, especially at high-demand intersections like WGM-AN, where 100% RVs achieve an 82.6% reduction. In contrast, the impact is minimal at lower-demand intersections like WGG-N. Travel times remain stable across scenarios, with notable improvements at WGM intersections. However, CO_2 emissions show mixed trends with the increase of RV penetration.

TABLE V

PERFORMANCE METRICS FOR MIXED TRAFFIC SCENARIOS WITH VARYING RV PENETRATION RATES ACROSS FOUR INTERSECTIONS. AT THE COMPLEX WGM INTERSECTION, WAIT TIMES SIGNIFICANTLY DROP. THE SIMPLER WGG INTERSECTION SHOWS SMALLER CHANGES. CO_2 EMISSIONS FOLLOW A NON-LINEAR TREND, REFLECTING TRADE-OFFS BETWEEN EFFICIENCY AND ENVIRONMENTAL IMPACT.

Scenario	Metric	HVs	RV Penetration Rate				
			20%	40%	60%	80%	100%
WGG-N	Wait Time (s)	**0.16**	0.19	0.27	0.44	0.47	0.41
	Travel Time (s)	83.82	84.38	84.79	86.08	86.25	86.22
	CO_2 Emissions (mg/s)	1642	1644	1640	1627	**1626**	1630
WGG-AN	Wait Time (s)	**0.78**	3.20	2.73	2.86	3.56	2.59
	Travel Time (s)	65.01	68.34	65.80	67.47	68.04	**64.61**
	CO_2 Emissions (mg/s)	3842	3405	3501	3424	**3350**	3529
WGM-N	Wait Time (s)	3.60	3.72	3.08	2.56	**1.52**	1.88
	Travel Time (s)	112.06	112.43	109.39	104.90	**99.72**	103.62
	CO_2 Emissions (mg/s)	1452	**1402**	1422	1443	1493	1470
WGM-AN	Wait Time (s)	16.21	2.11	1.71	1.98	1.72	**1.06**
	Travel Time (s)	127.36	98.86	98.16	100.44	99.00	**95.73**
	CO_2 Emissions (mg/s)	**1323**	1535	1537	1514	1527	1550

TABLE VI

PERFORMANCE METRICS AT WALNUT GROVE-GOODLETT UNDER INCREASED DEMAND. WITH 25% HIGHER DEMAND, 80% RV PENETRATION CUTS WAIT TIME FROM 6.48S TO 1.13S AND TRAVEL TIME FROM 95.53S TO 85.72S. AT 50% HIGHER DEMAND, IT REDUCES WAIT FROM 63.19S TO 33.47S AND TRAVEL FROM 166.97S TO 130.51S. CO_2 EMISSIONS RISE IN BOTH CASES.

Demand Increase	Metric	HVs	RV Penetration Rate				
			20%	40%	60%	80%	100%
25%	Wait Time (s)	6.48	7.81	4.15	2.33	**1.13**	3.06
	Travel Time (s)	95.53	97.14	91.48	88.44	**85.72**	90.47
	CO_2 Emissions (mg/s)	**1703**	1707	1759	1793	1825	1799
50%	Wait Time (s)	63.19	49.18	43.33	36.60	**33.47**	52.31
	Travel Time (s)	166.97	162.92	146.27	136.06	130.51	**129.39**
	CO_2 Emissions (mg/s)	**1440**	1489	1522	1565	1596	1864

with a 7.2% increase in CO_2 emissions. The benefits of RVs become even more pronounced with a 50% increase in traffic demand. RVs decrease the overall wait times by 47.1%, and travel times by 21.8%. As wait times decrease and throughput increases with higher RV penetration, we observe a corresponding increase in CO_2 emissions. This aligns with vehicles idling less and moving more at higher speeds, which generally leads to higher emission rates.

Overall, our analysis demonstrates that while RVs can significantly improve traffic efficiency during blackout, their effectiveness depends on factors such as traffic volume and penetration rate, highlighting the need for adaptive deployment strategies that balance traffic flow improvements with environmental considerations.

VII. CONCLUSION AND FUTURE WORK

We introduce Beacon, a naturalistic driving dataset collected during a blackout at two unsignalized intersections in Memphis, TN, USA. By analyzing and reconstructing traffic scenarios under unsignalized, signalized, and mixed traffic conditions, Beacon achieves high reconstruction accuracy (over 98% at simpler intersections) and serves as a valuable benchmark for advancing research in traffic reconstruction and control. Our results show the potential of robot vehicles (RVs) to improve traffic efficiency at high-demand intersections, reducing wait times by up to 82.6%, though CO_2 emissions vary with traffic density and penetration rates.

Challenges such as incomplete observations and human driver variability remain open. Future work will expand Beacon to include more intersections, varied scenarios, and longer timeframes, enabling broader use. We also plan to explore advanced reinforcement learning and adaptive reward functions to optimize traffic efficiency, safety, and sustainability. By addressing these challenges, Beacon aims to support the development of intelligent, resilient traffic management systems for complex real-world conditions.

REFERENCES

[1] A. Press, "Power still out to 50k customers, days after memphis storm," https://www.usnews.com/news/best-states/tennessee/articles/2022-02-07/power-still-out-to-60k-customers-days-after-memphis-storm, Feb. 2022.

[2] E.-H. Choi, "Crash factors in intersection-related crashes: An on-scene perspective," *National Highway Traffic Safety Administration, U.S. Department of Transportation*, 2010.

[3] B. Winck, "Get ready for blackouts from london to la, as the global energy crisis overwhelms grids and sends energy prices skyrocketing," https://www.businessinsider.com/global-europe-energy-crisis-power-electricity-outages-blackouts-energy-grid-2022-9, Sept. 2022.

[4] R. Ramirez, "Power outages are on the rise, led by texas, michigan and california. here's what's to blame," https://www.cnn.com/2022/09/14/us/power-outages-rising-extreme-weather-climate/index.html, Sept. 2022.

[5] M. Montanino and V. Punzo, "Trajectory data reconstruction and simulation-based validation against macroscopic traffic patterns," *Transportation Research Part B: Methodological*, vol. 80, pp. 82–106, 2015.

[6] E. R. Sanchez, S. Raghavan, and C. Wu, "Data-driven traffic reconstruction and kernel methods for identifying stop-and-go congestion," *arXiv preprint arXiv:2312.03186*, 2023.

[7] W. Li, D. Wolinski, and M. C. Lin, "City-scale traffic animation using statistical learning and metamodel-based optimization," *ACM Trans. Graph.*, vol. 36, no. 6, pp. 200:1–200:12, 2017.

[8] Y. Xu, W. Shao, J. Li, K. Yang, W. Wang, H. Huang, C. Lv, and H. Wang, "Sind: A drone dataset at signalized intersection in china," in *2022 IEEE 25th International Conference on Intelligent Transportation Systems (ITSC)*. IEEE, 2022, pp. 2471–2478.

[9] M. B. Jensen, A. Møgelmose, and T. B. Moeslund, "Presenting the multi-view traffic intersection dataset (mtid): A detailed traffic-surveillance dataset," in *2020 IEEE 23rd International Conference on Intelligent Transportation Systems (ITSC)*. IEEE, 2020, pp. 1–6.

[10] H. Yu, W. Yang, H. Ruan, Z. Yang, Y. Tang, X. Gao, X. Hao, Y. Shi, Y. Pan, N. Sun, *et al.*, "V2x-seq: A large-scale sequential dataset for vehicle-infrastructure cooperative perception and forecasting," in *Proceedings of the IEEE/CVF Conference on Computer Vision and Pattern Recognition*, 2023, pp. 5486–5495.

[11] Z. Shen, W. Ji, S. Yu, G. Cheng, Q. Yuan, Z. Han, H. Liu, and T. Yang, "Mapping the knowledge of traffic collision reconstruction: A scientometric analysis in citespace, vosviewer, and scimat," *Science & Justice*, vol. 63, no. 1, pp. 19–37, 2023.

[12] Q. Li, Z. M. Peng, L. Feng, Z. Liu, C. Duan, W. Mo, and B. Zhou, "Scenarionet: Open-source platform for large-scale traffic scenario simulation and modeling," *Advances in neural information processing systems*, vol. 36, 2024.

[13] P. Sun, H. Kretzschmar, X. Dotiwalla, A. Chouard, V. Patnaik, P. Tsui, J. Guo, Y. Zhou, Y. Chai, B. Caine, *et al.*, "Scalability in perception for autonomous driving: Waymo open dataset," in *Proceedings of the IEEE/CVF conference on computer vision and pattern recognition*, 2020, pp. 2446–2454.

[14] H. Caesar, V. Bankiti, A. H. Lang, S. Vora, V. E. Liong, Q. Xu, A. Krishnan, Y. Pan, G. Baldan, and O. Beijbom, "nuscenes: A multimodal dataset for autonomous driving," in *Proceedings of the IEEE/CVF conference on computer vision and pattern recognition*, 2020, pp. 11 621–11 631.

[15] M.-F. Chang, J. Lambert, P. Sangkloy, J. Singh, S. Bak, A. Hartnett, D. Wang, P. Carr, S. Lucey, D. Ramanan, *et al.*, "Argoverse: 3d tracking and forecasting with rich maps," in *Proceedings of the IEEE/CVF conference on computer vision and pattern recognition*, 2019, pp. 8748–8757.

[16] Q. Li, Z. Peng, L. Feng, Q. Zhang, Z. Xue, and B. Zhou, "Metadrive: Composing diverse driving scenarios for generalizable reinforcement learning," *IEEE Transactions on Pattern Analysis and Machine Intelligence*, 2022.

[17] A. Amini, T.-H. Wang, I. Gilitschenski, W. Schwarting, Z. Liu, S. Han, S. Karaman, and D. Rus, "Vista 2.0: An open, data-driven simulator for multimodal sensing and policy learning for autonomous vehicles," in *2022 International Conference on Robotics and Automation (ICRA)*. IEEE, 2022.

[18] "Autoware: Open-source software for urban autonomous driving," https://github.com/CPFL/Autoware, accessed: 2024-08-26.

[19] S. Bilotta and P. Nesi, "Traffic flow reconstruction by solving indeterminacy on traffic distribution at junctions," *Future Generation Computer Systems*, vol. 114, pp. 649–660, 2021.

[20] X. Qi, Y. Ji, W. Li, and S. Zhang, "Vehicle trajectory reconstruction on urban traffic network using automatic license plate recognition data," *IEEE Access*, vol. 9, pp. 49 110–49 120, 2021.

[21] A. Bakowski and L. Radziszewski, "Measurements of urban traffic parameters before and after road reconstruction," *Open Engineering*, vol. 11, no. 1, pp. 365–376, 2021.

[22] M. Čičić, M. Barreau, and K. H. Johansson, "Numerical investigation of traffic state reconstruction and control using connected automated vehicles," in *2020 IEEE 23rd International Conference on Intelligent Transportation Systems (ITSC)*. IEEE, 2020, pp. 1–6.

[23] C. Wu, A. R. Kreidieh, K. Parvate, E. Vinitsky, and A. M. Bayen, "Flow: A modular learning framework for mixed autonomy traffic," *IEEE Transactions on Robotics*, vol. 38, no. 2, pp. 1270–1286, 2022.

[24] B. Peng, M. F. Keskin, B. Kulcsár, and H. Wymeersch, "Connected autonomous vehicles for improving mixed traffic efficiency in unsignalized intersections with deep reinforcement learning," *Communications in Transportation Research*, vol. 1, p. 100017, 2021.

[25] Z. Yan and C. Wu, "Reinforcement learning for mixed autonomy intersections," in *IEEE International Intelligent Transportation Systems Conference*, 2021, pp. 2089–2094.

[26] D. Wang, W. Li, L. Zhu, and J. Pan, "Learning to control and coordinate hybrid traffic through robot vehicles at complex and unsignalized intersections," *arXiv preprint arXiv:2301.05294*, 2023.

[27] D. Wang, W. Li, and J. Pan, "Large-scale mixed traffic control using dynamic vehicle routing and privacy-preserving crowdsourcing," *arXiv preprint arXiv:2311.11347*, 2023.

[28] M. Villarreal, B. Poudel, J. Pan, and W. Li, "Mixed traffic control and coordination from pixels," *arXiv preprint arXiv:2302.09167*, 2023.

[29] B. Poudel, W. Li, and S. Li, "Carl: Congestion-aware reinforcement learning for imitation-based perturbations in mixed traffic control," *International Conference on CYBER Technology in Automation, Control, and Intelligent Systems (CYBER)*, 2024.

[30] B. Poudel, W. Li, and K. Heaslip, "Endurl: Enhancing safety, stability, and efficiency of mixed traffic under real-world perturbations via reinforcement learning," *IEEE/RSJ International Conference on Intelligent Robots and Systems (IROS)*, 2024.

[31] I. Islam, W. Li, S. Li, and K. Heaslip, "Heterogeneous mixed traffic control and coordination," *arXiv preprint arXiv:2409.12330*, 2024.

[32] W. I. S. E. Lab, "Waterloo multi-agent traffic dataset: Intersection," https://uwaterloo.ca/waterloo-intelligent-systems-engineering-lab/datasets/waterloo-multi-agent-traffic-dataset-intersection, 2021, accessed: 2025-07-13.

[33] OpenStreetMap contributors, "Openstreetmap," https://www.openstreetmap.org, 2013, accessed: 2023-03-25.

[34] P. A. Lopez, M. Behrisch, L. Bieker-Walz, J. Erdmann, Y.-P. Flötteröd, R. Hilbrich, L. Lücken, J. Rummel, P. Wagner, and E. Wießner, "Microscopic traffic simulation using sumo," in *The 21st IEEE International Conference on Intelligent Transportation Systems*. IEEE, 2018. [Online]. Available: https://elib.dlr.de/124092/

[35] M. Treiber, A. Hennecke, and D. Helbing, "Congested traffic states in empirical observations and microscopic simulations," *Physical review E*, vol. 62, no. 2, p. 1805, 2000.

[36] SUMO, "Hbefa3-based," 2024, accessed: 2025-02-12. [Online]. Available: https://sumo.dlr.de/docs/Models/Emissions/HBEFA3-based.html

[37] M. Wisal Khattak, A. Pirdavani, P. De Winne, T. Brijs, and H. De Backer, "Examining the effects of geometric features, traffic control, and traffic volume on crash frequency at urban intersections," in *International Conference on Transportation and Development 2020*. American Society of Civil Engineers Reston, VA, 2020, pp. 95–106.

[38] M. Hessel, J. Modayil, H. Van Hasselt, T. Schaul, G. Ostrovski, W. Dabney, D. Horgan, B. Piot, M. Azar, and D. Silver, "Rainbow: Combining improvements in deep reinforcement learning," in *AAAI Conference on Artificial Intelligence*, 2018.